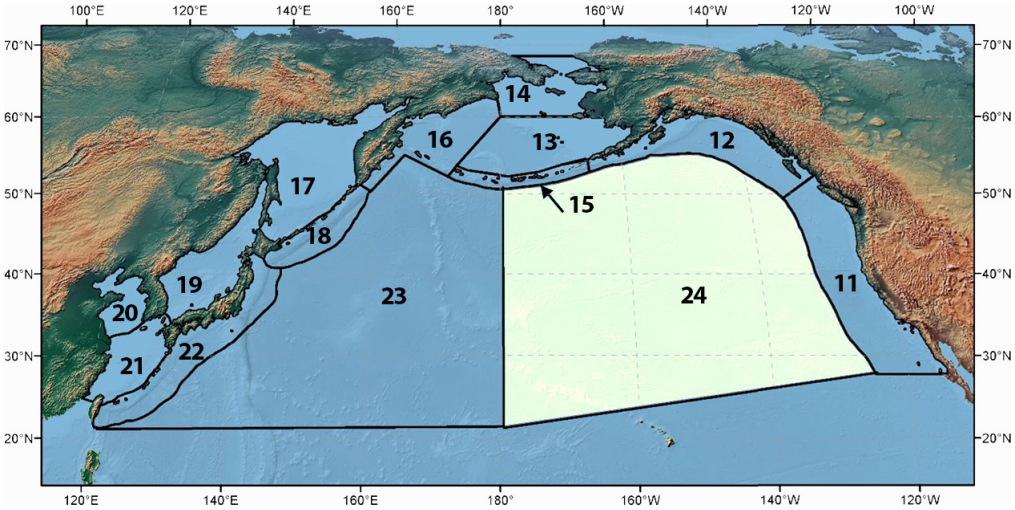

PICES

Regional Report for PICES Region: 24

PICES SPECIAL PUBLICATION 7

Marine Ecosystems of the North Pacific Ocean 2009–2016

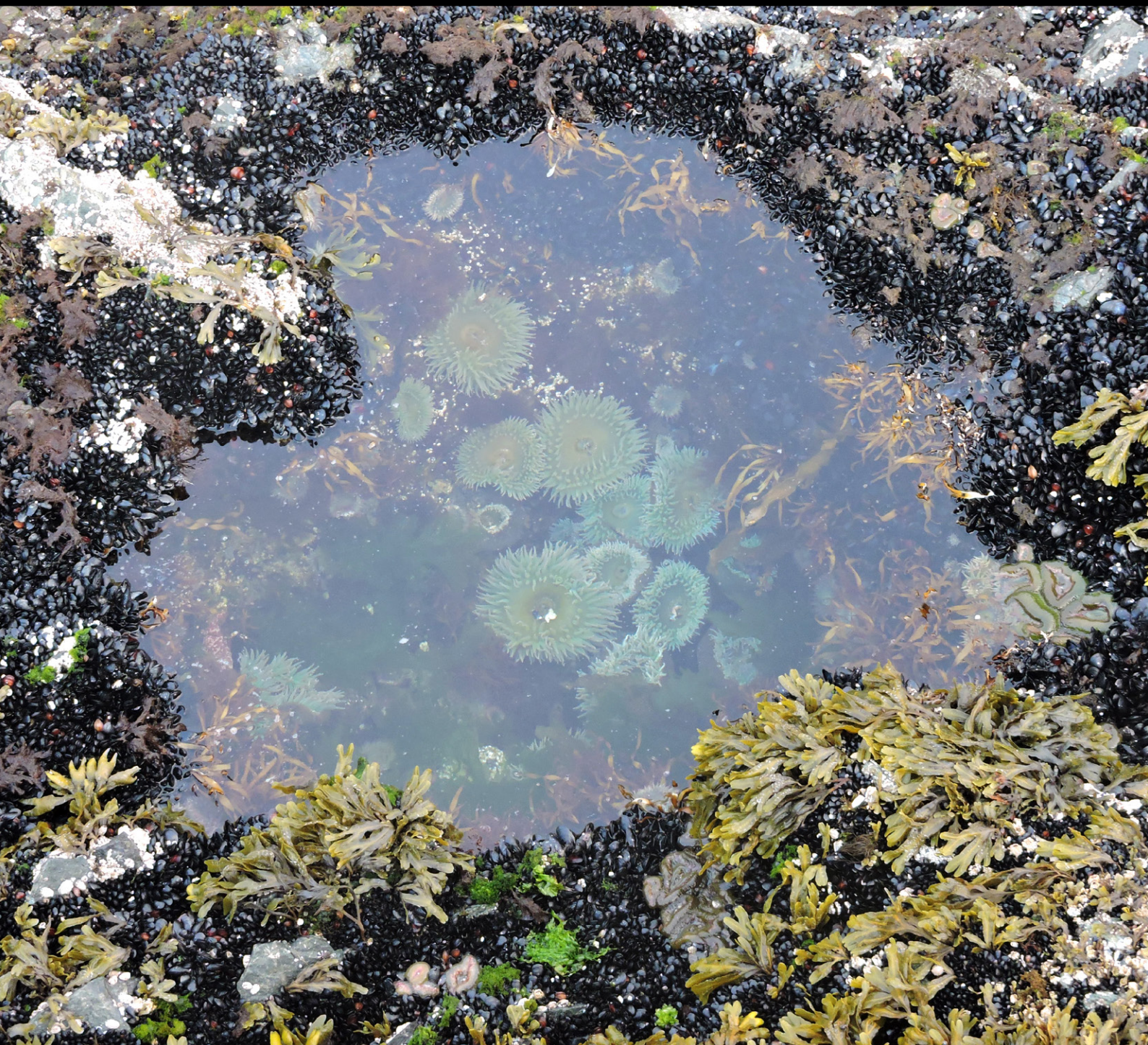

PICES North Pacific Ecosystem Status Report, Region 24 (Oceanic Northeast Pacific)

Sonia Batten

Marine Biological Association UK

Nanaimo, BC, Canada.

Contributors:

Marie Robert, Lisa Miller, Moira Galbraith, Angelica Peña, Tetjana Ross, Peter Chandler
Fisheries and Oceans Canada, Institute of Ocean Sciences, Sidney, BC, Canada

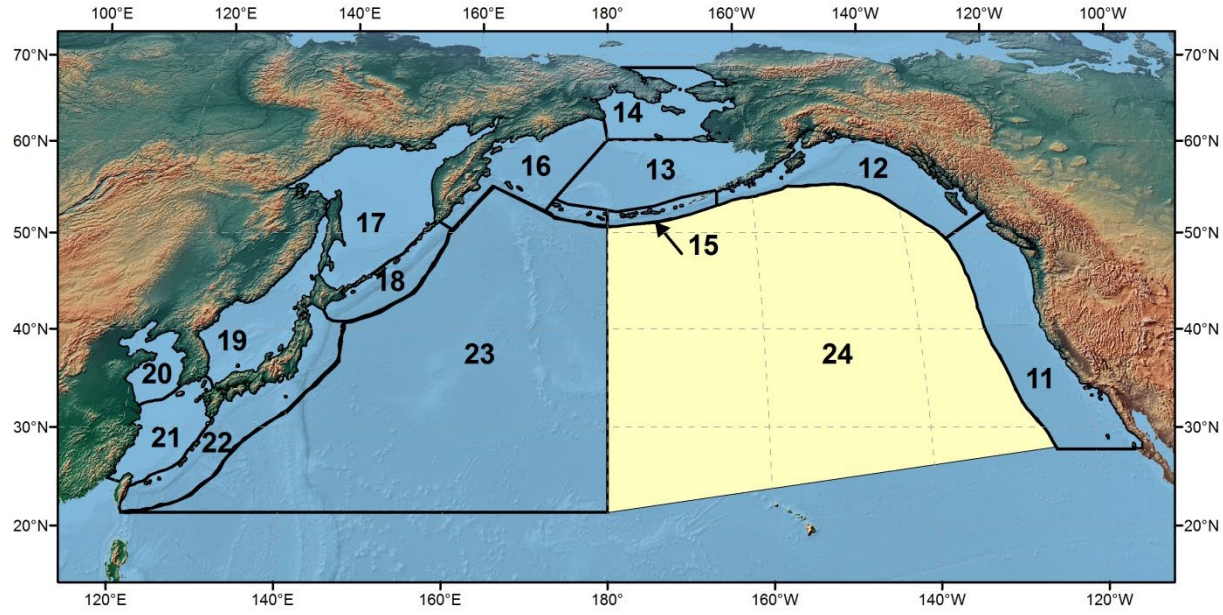

Figure R24-1. The PICES convention used to identify the areas included in the regional assessments for NPESR3, highlighting the region described in this chapter.

1. Highlights

The beginning of the focus period occurred while the Pacific Decadal Oscillation (PDO) Index was negative and conditions in Region 24 were cooler than average. The second half of the focus period, from the winter of 2013/14, experienced anomalously warm conditions, termed a marine heat wave, with positive PDO conditions and a strong El Niño.

Measurements at Ocean Station Papa (OSP) showed warmer than average surface conditions after 2013, especially striking in winter, with lower salinities and consequently stronger density gradients; winter mixing was therefore limited.

Nutrients were generally below average concentrations after 2013 and there was a likely reduction in larger phytoplankton taxa (mostly diatoms) during the marine heat wave of 2014–2016 so that the chlorophyll was predominantly made up of smaller cells.

Zooplankton abundances showed generally positive anomalies throughout the focus period but gelatinous plankton, taxa with a southerly distribution, and smaller copepods did especially well after 2013.

2. Introduction

Region 24 is the open ocean area of the Northeast Pacific (Figure R24-1) and includes the deep waters located beyond the continental margin and major coastal boundary currents. It is characterized by strong latitudinal gradients in surface temperature and salinity, an oceanic gyre, large (~200 km) mesoscale eddies, and a bathymetry which includes remote sea mounts. The Aleutian Island chain constricts the main North Pacific gyre and causes a re-circulation as the Alaskan Gyre. To the south is the North Pacific Transition Zone which contains waters of both subarctic and subtropical origin and which represents a physical and biological transition between the subtropical and subarctic gyres. The region is considered to be iron-limited and thus a High Nutrient Low Chlorophyll (HNLC) region with generally sufficient nitrate to support phytoplankton growth if iron were not limiting. Natural variability in the oceanic region is intimately linked to variability in the global climate system. Biological production in this region is a source of major commercial fisheries for tunas and Pacific salmon.

The region is relatively poorly sampled, especially for parameters beyond physical, chemical and lower trophic levels, and data contributed for this region come from measurements made by the Line P program (outer stations P12 to P26) operated by Fisheries and Oceans Canada and by the North Pacific Continuous Plankton Recorder (CPR) Survey (Figure R24-2). These programs are supplemented by data from satellites and the Argo program which cover the wider area.

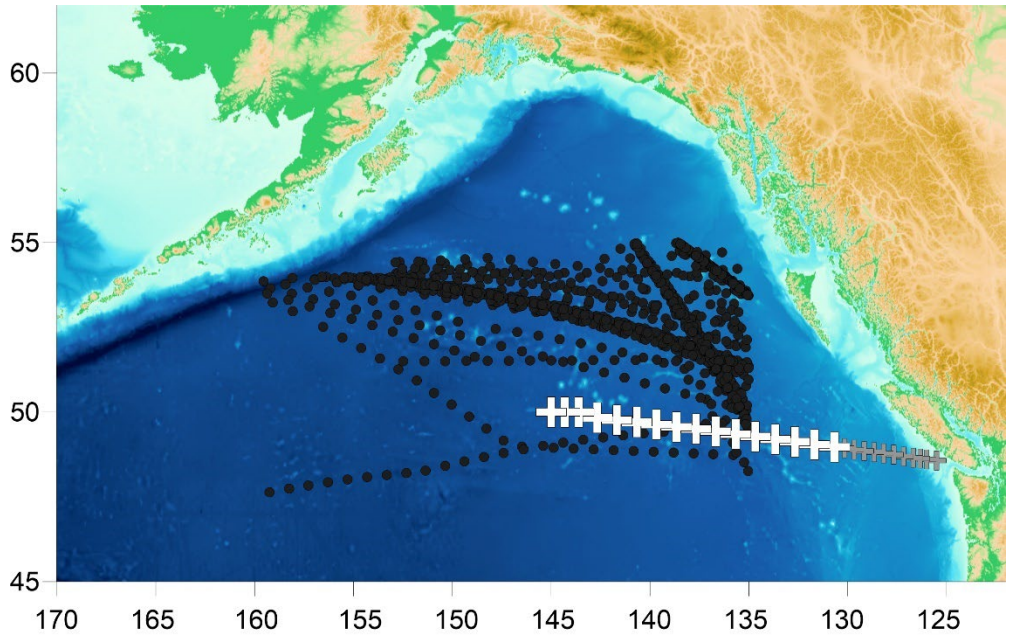

Figure R24-2. Location of data sources for Region 24. Solid black circles show the CPR samples and +s show the Line P sampling stations (Stations 12 to 26 are in white).

3. Climate

The section by Bond (Chapter 2 in Chandler and Yoo, 2021) describes the ocean climate of the entire North Pacific for the focus period (2009–2016) of this report. The climate of the oceanic Northeast Pacific for this period essentially comprised two different halves, with sea surface temperatures (SST) cooler than average from 2009 to 2012 and warmer than average from 2014 to 2016 (Figure 3-4, Chandler and Yoo, 2021). The Pacific Decadal Oscillation (PDO) Index (Mantua et al., 1997) represents the dominant mode of variability in SST for the North Pacific. The PDO is derived from the dominant eigenvector of the covariance matrix of area-weighted monthly anomalies of SST from 20°N–65°N in the Pacific and is shown in Figure R24-3. During the past two decades the PDO Index has varied between positive and negative states with greater frequency than was observed at the time of its first description (approximately 5-year stanzas instead of decadal-scale oscillations). From 2009 to the end of 2013 the index remained mostly negative but became positive early in 2014, in conjunction with a marine heat wave and El Niño (Di Lorenzo and Mantua, 2016), and remained positive for the rest of the focus period.

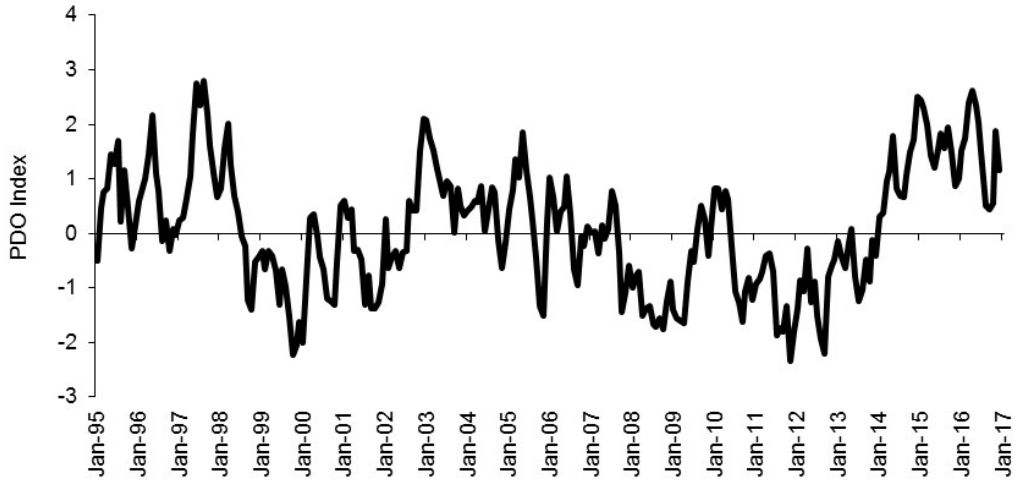

Figure R24-3. Time series of monthly Pacific Decadal Oscillation (PDO) values, 1995 to 2016, from http://research.jisao.washington.edu/pdo/PDO.latest.txt.

The North Pacific Gyre Oscillation (NPGO) represents the second leading mode of sea surface height (SSH) variability in the North Pacific. Di Lorenzo et al. (e.g., 2008) have shown that the NPGO is related to a variety of physical and biochemical ocean variables in the Northeast Pacific. This index also showed the two distinct halves of the focus period with positive values of the NPGO prevailing from 2009 through most of 2013, which corresponds to relatively cool SST across the North Pacific north of about 40°N. The NPGO shifted to a negative state in late 2013, with this state persisting through 2015. This period coincides with relatively warm upper ocean temperatures in much of the Northeast Pacific. The NPGO was near zero as a whole for 2016.

4. Physical Ocean

4.1. Water Properties from Line P

(Robert, M.)

The Line P program began in 1959 when hydrographic casts were made at a series of stations along a transect leading to Ocean Station Papa (OSP) at 50°N, 145°W (Freeland, 2007). This is one of the longest deep-ocean time series in existence and is now sampled 2–5 times per year by the Canadian Department of Fisheries and Oceans (Fisheries and Oceans Canada), usually in late winter (February/March), spring (May/June) and summer (August/September). Data shown here are from OSP (station P26) and data from the landward station P16 (49°17'N, 134°40'W, water depth 3550 m) were also available, but not shown.

Between 1993 and 1996, inclusively, the CTD data (pressure, temperature, salinity) were collected using a Guildline Model CTD. From 1997 to present the CTD data were collected using a Seabird 911plus model. Temperature profiles for each season and each year at OSP

are plotted in Figure R24-4, together with the mean for 1993 to 2008. 2014 and 2015 were consistently warmer in the surface 100 m than the long-term mean and this was particularly striking in the winter.

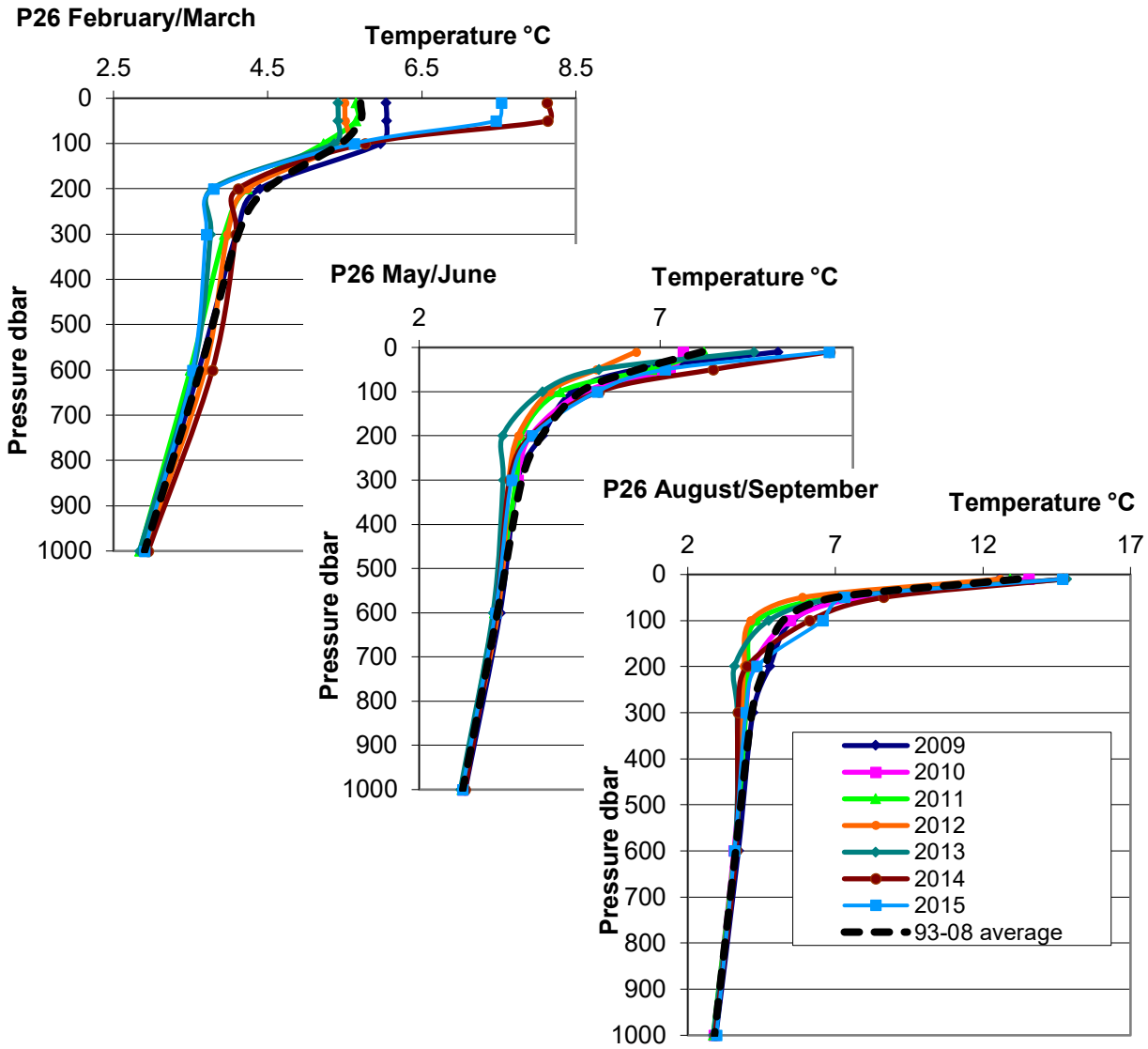

Figure R24-4. Temperature profiles at OSP (P26) for three seasons. Each year of the focus period is shown, together with the mean for 1993–2008.

The salinity profiles for station P26 are shown in Figure R24-5. Surface waters were fresher than average in 2014 and 2015 in all three seasons.

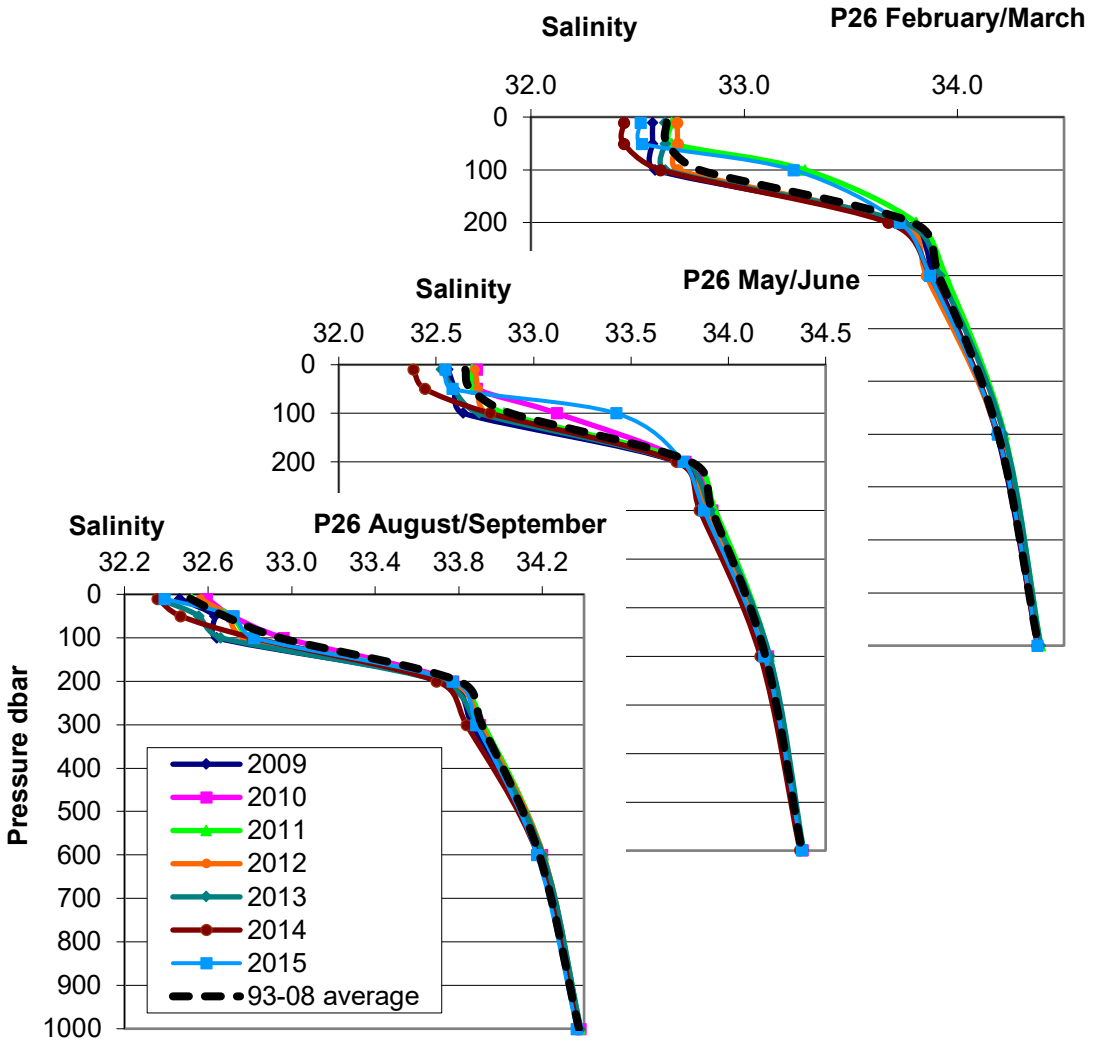

Figure R24-5 Salinity profiles at OSP (P26) for three seasons. Each year of the focus period is shown, together with the mean for 1993–2008.

The warm temperatures and fresher water resulted in least dense surface waters in 2014 in all three seasons, although 2015 was also less dense than average. The differences at depth were not so large, therefore, the strongest gradients between surface and deeper waters also existed in 2014 and 2015.

4.2. Winter Mixing

(Ross, T.)

Figure R24-6 shows a time-series of the 1025.7 kg/m^3 isopycnal depth at Station P (Ocean Station Papa/P26), based on Argo data. To compile the time series, all Argo profiles of temperature and salinity collected in a calendar month were optimally interpolated to create a monthly mean profile at the location of Station P. Then, density was calculated and the depth at which the water was 1025.7 kg/m^3 in the monthly profile (i.e., the depth of the isopycnal) was

determined. The 1025.7 kg/m^3 isopycnal is an index of mixing intensity, as it reaches close to the surface in winter when mixing is good and it stays deeper in poor mixing years.

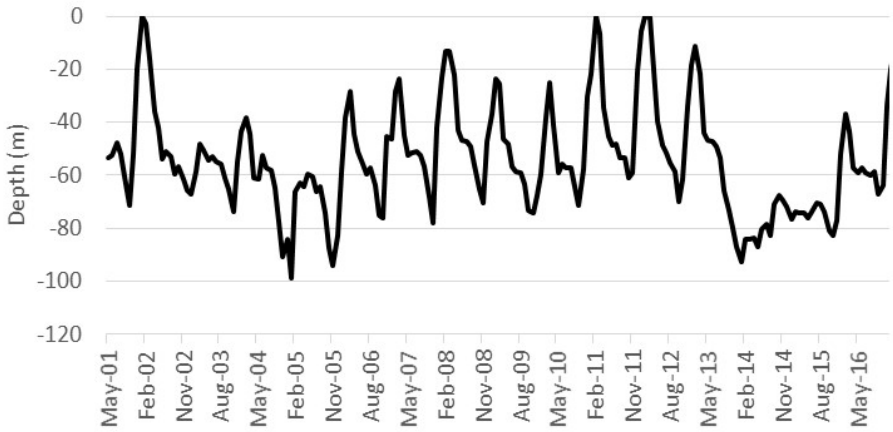

Figure R24-6. Monthly depth (m) of the 1025.7 kg/m^3 isopycnal at Station P, from Argo data, http://doi.org/10.17882/42182. These data were collected and made freely available by the International Argo Program and the national programs that contribute to it (http://argo.jcommops.org). The Argo Program is part of the Global Ocean Observing System.

The time series shows that in the winters of 2011 and 2012 the isopycnal reached right to the surface, indicating strong winter mixing. In 2014–2015, the isopycnal remained very deep and its depth did not vary during winter, suggesting that mixing was very limited.

4.3. Mixed Layer Depth

(Chandler, P.)

Mixed Layer Depth (MLD) was calculated from Argo float profiles, averaged for all floats reporting data within the region shown in Figure R24-1 each month. The MLD is strongly seasonal with maximum depth in February/March each year and a minimum depth in July/August. Figure R24-7 shows the monthly MLD with the mean seasonal cycle removed to show any trends. Between 2004 and 2009 there was an increasing trend in MLD, followed by strong variability in the first few years of the current focus period and then reduced MLD from late 2013 through 2015, consistent with the winter mixing reduction described in the previous section. This supports the view that the marine heatwave has a wide spatial influence.

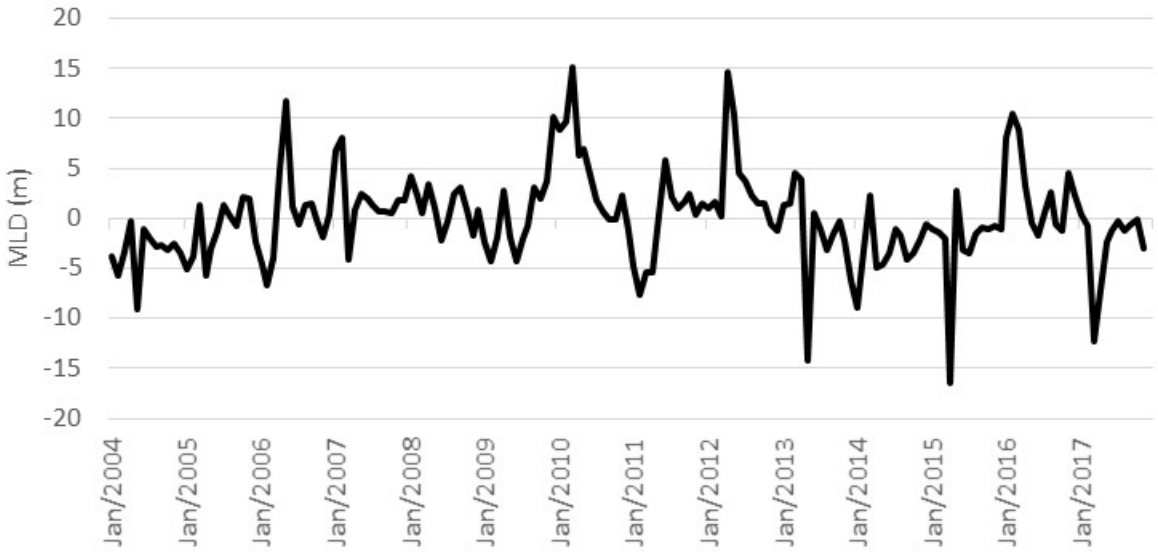

Figure R24-7. Mixed Layer Depth from all Argo floats within Region 24, seasonal cycle removed.

5. Chemical Ocean

5.1. Nutrients at OSP

(Robert, M.)

All dissolved nutrient samples were collected during the focus period using a CTD/Rosette package. Data from 10, 50, 100, 200, 300, 600, and 1000 dbar (± 10 dbar) comprise the dataset. If more than one cast was performed at one station during the time period, the average of all data was computed so that each 2-month period has the same weight. Most nutrient samples were analyzed from frozen samples returned to the lab. Exceptions were all samples from 2009, winter 2010, autumn 2011 and summer 2012, which were analysed fresh on board using a Technicon AAII or Astoria auto-analyzer following methods described in Barwell-Clarke and Whitney (1996). Table R24-1 lists the nutrient profiles for OSP (station P26) in each of three seasons for each year of the focus period, together with the long-term mean (1993–2008).

Table R24-1. Nutrient profiles at OSP µmol L^{-1}. Depth is from nominal pressure. LT (Long Term) Mean values are from 1993–2008.

Nitrate plus Nitrite

	Spring (Feb-Mar)								Summer (May-Jun)								Autumn (Aug-Sep)							
Depth (m)	**LT Mean**	2009	2010	2011	2012	2013	2014	2015	**LT Mean**	2009	2010	2011	2012	2013	2014	2015	**LT Mean**	2009	2010	2011	2012	2013	2014	2015
10	**14**	14		14	17	17	11	11	**12**	10	12	13	16	13	9	9	**8**	7	8	11	11	10	5	6
50	**14**	15		14	17	17	11	12	**13**	12	12	16	16	17	11	14	**12**	11	12	17	17	14	10	13
100	**17**	16		17	17	17	12	23	**18**	15	20	20	17	20	20	24	**19**	15	18	21	20	19	18	17
200	**35**	34		40	35	39	35	39	**35**	34	36	37	37	38	36	37	**35**	30	36	38	38	40	37	36
300	**40**	40		43	40	43	38	44	**40**	42	40	41	41	43	42	42	**40**	40	41	41	42	44	43	41
600	**44**	45		45	44	44	46	45	**44**	45	45	44	43	44	46	45	**44**	44	41	44	44	45	45	45
1000	**45**	46		45	46	45	47	46	**45**	46	45	46	45	44	46	46	**45**	45	46	44	45	46	46	46

Phosphate

	Spring (Feb-Mar)								Summer (May-Jun)								Autumn (Aug-Sep)							
Depth (m)	**LT Mean**	2009		2011	2012	2013	2014	2015	**LT Mean**	2009	2010	2011	2012	2013	2014	2015	**LT Mean**	2009	2010	2011	2012	2013	2014	2015
10	**1.3**	1.4		1.3	1.5	1.5	1.1	1.1	**1.2**	1.1	1.2	1.2	1.4	1.3	1.0	1.0	**0.9**	0.8	0.9	1.2	1.1	1.0	0.7	0.7
50	**1.3**	1.4		1.3	1.5	1.4	1.1	1.1	**1.3**	1.3	1.2	1.5	1.5	1.5	1.1	1.3	**1.3**	1.2	1.2	1.5	1.5	1.3	1.1	1.2
100	**1.5**	1.5		1.5	1.5	1.5	1.1	1.7	**1.6**	1.4	1.6	1.7	1.6	1.7	1.6	1.8	**1.6**	1.4	1.5	1.7	1.6	1.6	1.5	1.4
200	**2.5**	2.6		2.9	2.5	2.8	2.4	2.7	**2.5**	2.5	2.7	2.7	2.7	2.7	2.5	2.6	**2.6**	2.3	2.6	2.8	2.7	2.9	2.6	2.5
300	**2.9**	3.0		3.0	2.9	3.1	2.6	3.0	**2.9**	3.0	2.9	2.9	3.0	3.0	2.9	2.9	**2.9**	2.9	2.9	3.0	3.0	3.1	3.0	2.8
600	**3.2**	3.3		3.2	3.1	3.2	3.1	3.1	**3.1**	3.2	3.2	3.2	3.2	3.1	3.2	3.1	**3.2**	3.2	3.1	3.2	3.1	3.2	3.1	3.1
1000	**3.2**	3.4		3.3	3.3	3.2	3.2	3.1	**3.2**	3.3	3.2	3.2	3.3	3.2	3.2	3.2	**3.2**	3.3	3.2	3.3	3.2	3.2	3.2	3.2

Silicate

	Spring (Feb-Mar)								Summer (May-Jun)								Autumn (Aug-Sep)							
Depth (m)	**LT Mean**	2009		2011	2012	2013	2014	2015	**LT Mean**	2009	2010	2011	2012	2013	2014	2015	**LT Mean**	2009	2010	2011	2012	2013	2014	2015
10	**6**	21		19	27	25	13	13	**18**	17	17	20	27	25	14	14	**13**	12	14	16	22	18	12	11
50	**20**	21		20	27	25	13	14	**20**	19	17	24	27	28	15	21	**18**	16	17	27	30	22	14	20
100	**25**	23		24	27	26	15	32	**27**	22	30	31	29	31	27	36	**29**	21	26	33	34	28	23	24
200	**66**	64		76	64	77	61	74	**66**	64	69	72	70	74	64	69	**66**	54	68	74	73	75	68	67
300	**83**	83		91	83	93	78	90	**84**	87	84	86	88	91	83	87	**83**	80	86	89	90	92	86	84
600	**118**	120		125	114	124	116	124	**118**	123	122	121	118	121	119	120	**119**	118	121	119	120	118	117	120
1000	**145**	150		148	143	149	143	146	**147**	151	148	145	144	146	143	147	**146**	145	146	142	146	146	141	144

Surface/near-surface nutrients showed a consistent grouping of years with concentrations of all three nutrients tending to be above average in 2012–2013 and below average in 2014–2015, particularly in spring and summer. The earlier years were more variable but not generally as far from the long-term mean.

5.2. Dissolved Oxygen at OSP

(Robert, M.)

All dissolved oxygen samples were collected during the focus period using a CTD/Rosette package. Data from 10, 50, 100, 200, 300, 600, and 1000 dbar (± 10 dbar) comprise the dataset. If more than one cast was performed at one station during the time period, the average of all data was computed so that each 2-month period has the same weight. Oxygen samples were analyzed at sea until February 2015 using an automated Winkler titration system following the procedures of Carpenter (1965). A Brinkmann model 665 Dosimat and model PC910 Colorimeter were controlled by a Visual-Basic program to titrate the oxygen samples. From summer 2015 onwards the system used was a Metrohm Dosimat model 876 and a UV light source and detector with a 365 nm filter controlled by LV02_876 software designed and constructed by Scripps Institution of Oceanography, with modifications based on Carpenter (1965) and adhering to WOCE protocols (Culberson, 1991).

Declining oxygen levels in sub-surface waters of the subarctic Pacific have been noted (Whitney et al., 2007). In the plots below, most of the years of the focus period (Figure R24-8) show a spread around the long-term mean at depth, but near-surface concentrations in spring and summer were typically below average, with the exception of 2012 (summer) and 2013 (spring).

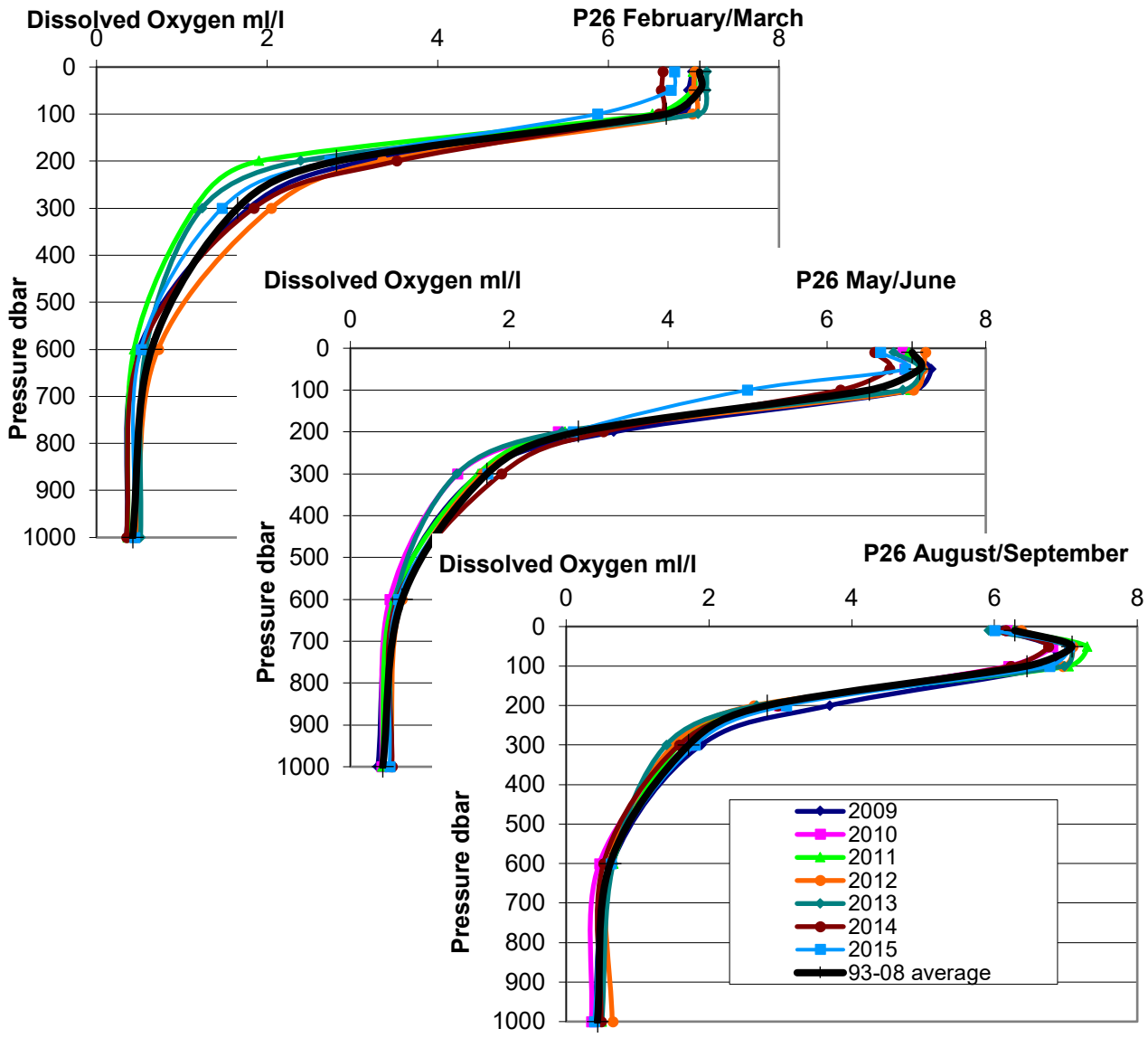

Figure R24-8. Oxygen profiles at OSP (P26) for three seasons. Each year of the focus period is shown, together with the mean for 1993–2008.

5.3. pH at OSP

(Miller, L.)

The time series of directly measured pH from OSP is still too short to confidently address the question of whether or not there is a long-term declining trend in pH which would confirm the expectation that increased global emissions of CO_2 are causing an acidification of the ocean. However, data collected during the focus period are presented here. Discrete samples were collected from the CTD-rosette directly into 10-cm spectrophotometric cells and were analyzed on board for pH. The analyses were conducted spectrophotometrically, using standard protocols (Dickson et al., 2007). Precision varied between cruises, ranging from 0.001 to 0.003, and

accuracy was confirmed by comparison with measured dissolved inorganic carbon and total alkalinity. The depth axis (and colour scale) in the plot in Figure R24-9 has been skewed to emphasise the Oxygen Minimum Zone. There is perhaps a slight deepening trend in lower pH over the focus period, but essentially the profiles show that pH is very variable at OSP, particularly in the pycnocline and in the OMZ.

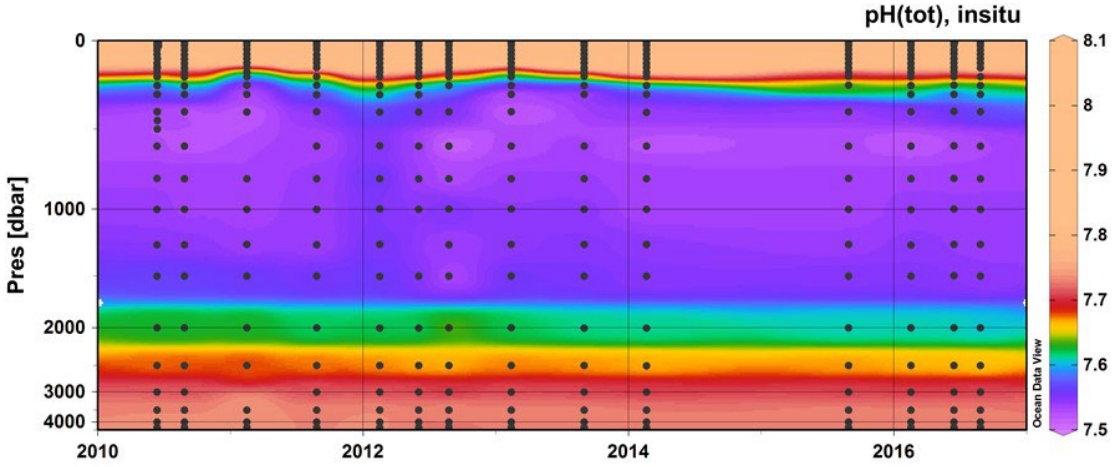

Figure R24-9. Measured pH at OSP, corrected to in-situ temperature and pressure, using an average total inorganic carbon value of 2250 µmol/kg.

6. Phytoplankton

6.1. Chlorophyll a at OSP

(Peña, A.)

Chlorophyll concentrations are usually low (<0.5 mg m^{-3}) and show little seasonal variability in the eastern subarctic Pacific. Ship-based observations at OSP (Figure R24-10) show that chlorophyll concentrations in winters/early springs of the focus period were above average, except for 2014. Summer surface concentrations were also generally above average, again except for 2014. The late summer/autumn profiles were distributed around the long-term mean, although in this season 2014 was noticeably higher than average.

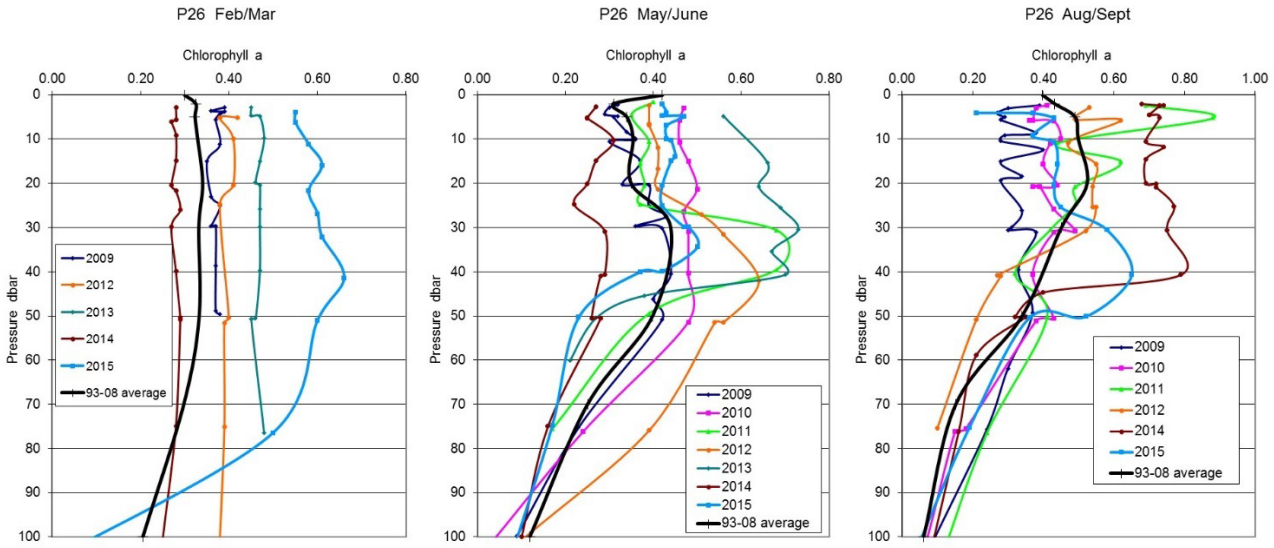

Figure R24-10 Chlorophyll a (mg m^{-3}) profiles at OSP (P26) for three seasons. Each year of the focus period is shown, together with the mean for 1993–2008.

6.2. Chlorophyll a from MODIS

(Chandler, P.)

Time series of MODIS chlorophyll a data were created for four locations across Region 24 from the MODIS-Aqua Level-3 Mapped Chlorophyll Data Version 2018. Figure R24-11 shows the chlorophyll a concentration averaged over a 1° x 1° area centred on the geographic location given in each panel. These graphs show the regional variability of phytoplankton density across the larger oceanic area with slightly higher values and no seasonality to the north and stronger seasonality to the south. The lack of seasonality in the north is likely due to iron limitation in the High Nutrient Low Chlorophyll (HNLC) region. There are a few peaks in the time series, limited mostly to the southwestern box, which may be an artefact of the data, otherwise all regions show no long-term trend. The start of the focus period saw relatively high values in 2009–2010 which then declined somewhat by 2012 before showing a slight increase through 2015–2016 in all four regions, consistent with the mostly higher than average profiles at OSP.

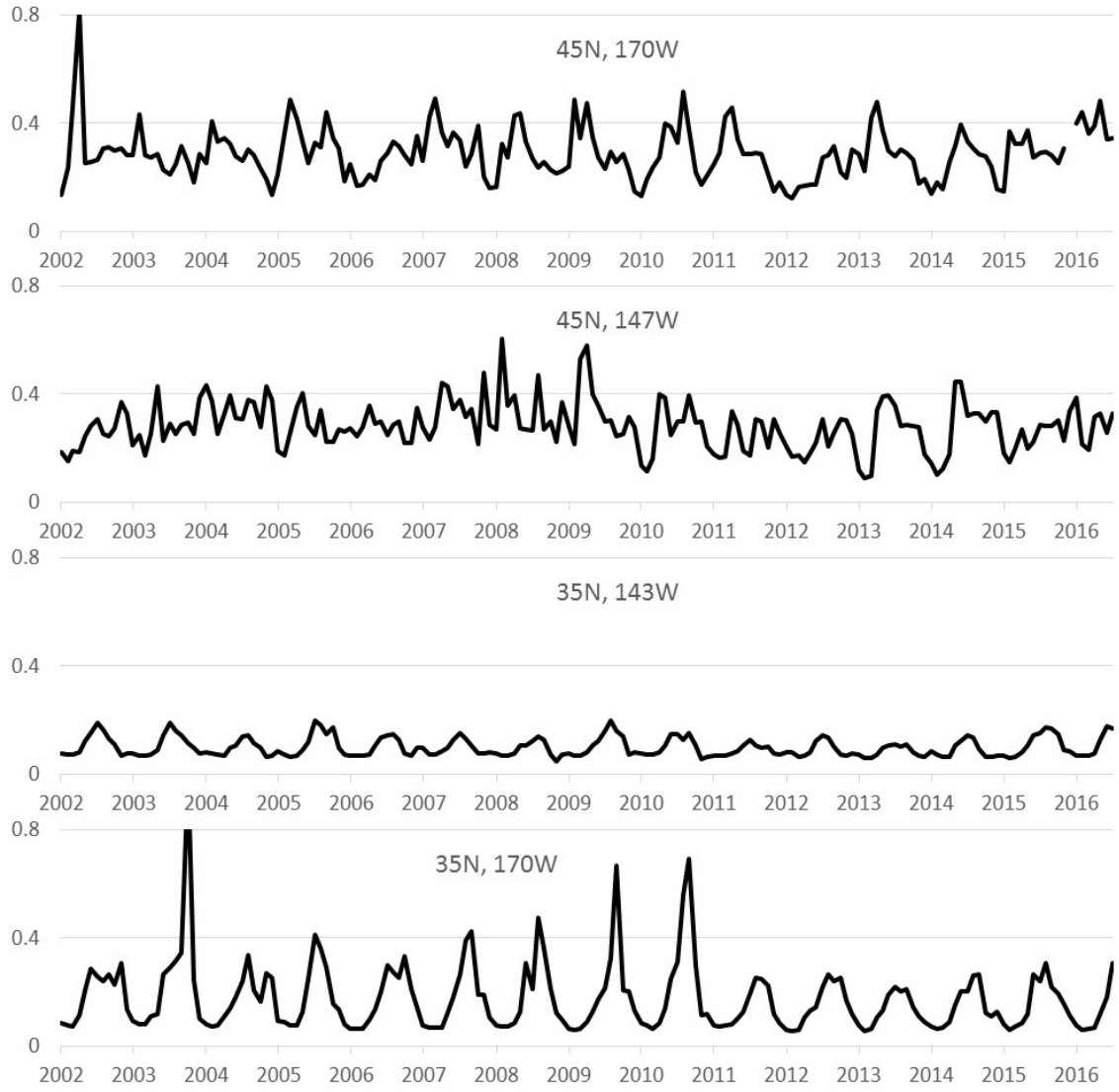

Figure R24-11. Mean monthly chlorophyll a values (mg m^{-3}) from MODIS-Aqua for a 1° x 1° box centred at the location given in each panel.

6.3. Phytoplankton composition at OSP

(Peña, A.)

The contribution of the main taxonomic groups of phytoplankton to total chlorophyll a were determined from phytoplankton pigment samples (chlorophylls and carotenoids) measured by high performance liquid chromatography (HPLC) followed by CHEMTAX analysis (Mackey et al., 1996). The phytoplankton assemblage (Figure R24-12) was diverse, with haptophytes being usually the most abundant phytoplankton group. The contribution of the other phytoplankton groups was variable and showed no consistent seasonal variability. High chlorophyll concentrations in August 2008 and June of 2016 were mostly due to an increase in

diatom abundance. The increase in phytoplankton abundance in 2008 was most likely due to an increase in iron availability after a volcanic eruption in the Aleutian Islands (Hamme et al., 2010).

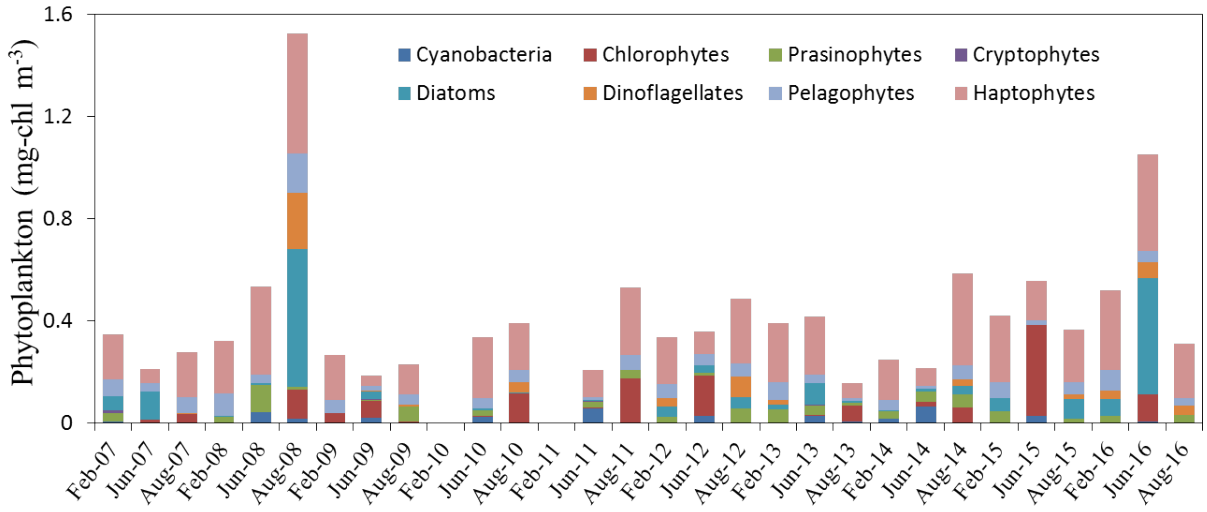

Figure R24-12. Phytoplankton composition at OSP measured from high performance liquid chromatography (HPLC) pigment analysis of samples collected in February, June, and August for each year from 2007 to 2016.

6.4. Phytoplankton abundance

(Batten, S.)

Continuous Plankton Recorder (CPR) data available from the samples shown in Figure R24-2 were collected between March and October each year (see Batten et al., 2003 for sampling methods). The vast majority of the phytoplankton cells retained and identified from the samples were larger diatoms; individual taxa counts were summed and used to calculate total diatom monthly means for the entire region, shown in Figure R24-13.

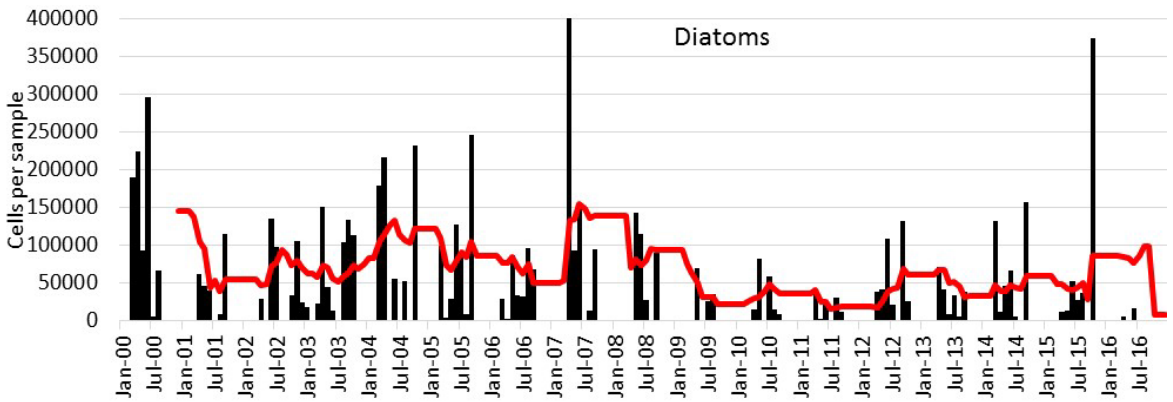

Figure R24-13. Mean monthly diatom abundance (bars) per Continuous Plankton Recorder (CPR) sample (approximately 3 m^3). Red line shows a 12-point running mean to indicate the trend.

Diatoms were generally lower in the years after 2008 than in the period before, until autumn 2015 when there was a high month. It is not certain whether this suggests less productivity during the focus period, or that there was a greater abundance of smaller cells not well sampled by the CPR instead. Since chlorophyll a values were mostly elevated in the focus period (Figures R24-10 and 11), it is more likely that there were was a greater abundance of smaller cells. This result suggests that the phytoplankton base of the food chain was somewhat different in 2009–2015.

7. Zooplankton

7.1. Mesozooplankton abundance and composition

(Galbraith, M. and Batten, S.)

Two sources of zooplankton information are available from the CPR samples shown in Figure R24-2 and from stations along Line P. Net sampling has been conducted along Line P in a routine way (two to three seasons per year) since 1997 and data for the outer stations (P16, P20 and P26/OSP) for key taxonomic groups are presented in Figure R24-14 as annual anomalies. To describe interannual variability from this dataset, the approach has been to calculate within each year a regional, logarithmic-scale biomass anomaly for each species and for each month that was sampled in a given year. The monthly anomalies in each year are then averaged to give an annual anomaly (Mackas et al., 2001).

Figure R24-14. Annual anomalies of zooplankton groups from Line P stations P16, P20 and P26. Anomalies are averaged for contributing taxa and calculated against a 1980–2005 climatology.

Subarctic copepods are typically large species (several mm in length) with a one-year life cycle that includes a dormancy period at depth during winter. They accumulate lipids as a reserve while in surface waters in spring and summer, and are thus a nutritional food source for predators. At the start of the focus period their numbers were positive, following the transition to cooler conditions that occurred in 2007/08 (Figure R24-4) but towards the end of the period (2014) numbers declined. At the same time numbers of smaller (<2 mm) southern species increased, associated with the marine heat wave of 2014–2016 which favoured their northwards expansion. Chaetognaths (predatory arrow worms) also showed a similar pattern from 2014 onwards, with southern species relatively more abundant and northern species becoming less common. Other groups that also showed an increase at this time were mostly gelatinous taxa such as the urochordates (salps, doliolids and larvaceans) and pteropods (three genera are

shown: Limacina, Clionidae, and Clio). Consequently, while crustacean zooplankton showed positive anomalies throughout the focus period, the more recent years (2014–2016) were characterised by a strong increase in gelatinous plankton. We can speculate that the above-average chlorophyll levels and likely bias towards smaller phytoplankton species described above favours those gelatinous zooplankton organisms that feed using mucous which can trap smaller particles.

The CPR does not sample all gelatinous plankton sufficiently quantitatively, so the mesozooplankton abundance time series shown in Figure R24-15 is the combined abundance of all zooplankton taxa recorded per sample (except ciliates and eggs of copepods / euphausiids / fish). While it includes chaetognaths, pteropods, larvaceans, etc., it is dominated by crustacean plankton. The time series “Average Copepod Community Size” is defined as:

$$\overline{S} = \frac{\sum_{i=1}^{N}(L_i \times X_i)}{\sum_{i=1}^{N} X_i}$$

where for each sample, the length L (in mm) of each copepod species i (adult female length), is multiplied by its abundance X_i, summed over all species (N) and divided by the total abundance, according to Beaugrand et al. (2003). Copepod size is an indicator of the community bias towards larger, typically subarctic species or smaller, typically more southern species.

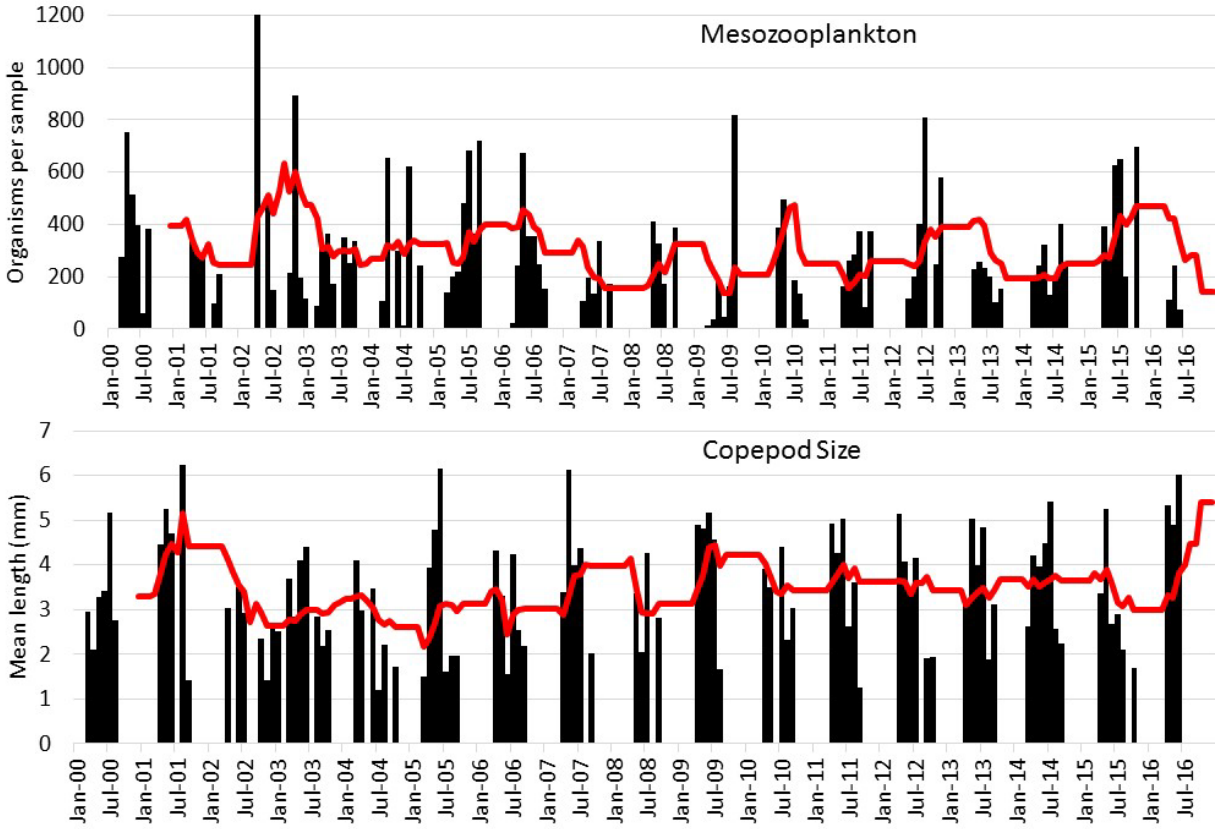

Figure R24-15 Mean monthly mesozooplankton abundance (top) per CPR sample (approximately 3 m^3) and mean copepod size (bottom). Red line shows a 12-point running mean to indicate the trend.

There is no apparent trend in mesozooplankton abundance, with numbers during the focus period similar to numbers in the preceding years. Copepod size was somewhat reduced during 2011–2015 compared to the high point of 2008–2009 but it was not as low as during the previous warm phase of 2004–2005. This is in agreement with the Line P net sampling results in Figure R24-14, where subarctic copepods species showed positive anomalies during the focus period. While smaller species were more common during the marine heat wave than before it, the community also contained larger species so that the mean size was not substantially reduced.

8. Climate Change, Ecosystem Considerations and Emerging Issues

The marine heat wave of 2014–2016 dominated this focus period and likely overwhelmed subtler trends related to long-term climate change in the time series considered here. Nevertheless, the extended period of warmth did reveal some likely consequences of a future warmer ocean. Peña et al. (2019) summarise how the increased warmth in the oceanic region increased stratification and so reduced the replenishment of surface nutrients in winter. Phytoplankton biomass was then affected with an increase in cyanobacteria. The zooplankton sampling described above showed an increase during the heatwave in southern copepod taxa, which are typically smaller in size. While crustacean zooplankton biomass did not change dramatically, there was a significant increase in gelatinous plankton during the heat wave, including those taxa (e.g., larvaceans, Figure R24-14) that are able to consume very small particles. These changes suggest that there was almost certainly a change in the ecosystem functioning during the latter part of the focus period. The physical conditions promoted a food chain that relied on smaller phytoplankton that could be successful under lower nutrient conditions, followed by a greater abundance of smaller copepods and gelatinous zooplankton able to utilise these cells. It is likely that there will be consequent impacts on longer-lived higher trophic levels that forage in this region, which may be evident in the next focus period.

9. References

Barwell-Clarke, J. and Whitney, F. 1996. Institute of Ocean Sciences Nutrient Methods and Analysis. Can. Tech. Rep. Hydrogr. Ocean Sci., No. 182, 43 pp.

Batten, S.D., Clarke, R.A., Flinkman, J., Hays, G.C., John, E.H., John, A.W.G., Jonas, T.J., Lindley, J.A., Stevens, D.P., and Walne, A.W. 2003. CPR sampling – The technical background, materials and methods, consistency and comparability. Prog. Oceanogr. 58: 193–215, https://dx.doi.org/10.1016/j.pocean.2003.08.004

Beaugrand, G., Brander, K.M., Lindley, J.A., Souissi, S., and Reid, P.C. 2003. Plankton effect on cod recruitment in the North Sea. Nature 426: 661–664, https://doi.org/10.1038/nature02164

Carpenter, J.H. 1965. The Chesapeake Bay Institute technique for the Winkler dissolved oxygen method. Limmnol. Oceanogr. 10: 141–143, https://doi.org/10.4319/lo.1965.10.1.0141

Chandler, P.C. and Yoo, S. (Eds.) 2021. Marine Ecosystems of the North Pacific Ocean 2009–2016: Synthesis Report, PICES Special Publication 7, 82 pp.

Culberson, C.H. 1991. Dissolved oxygen. WOCE Operations Manual. Vol. 3, Sect. 3.1, Part 3.1.3: WHP Operations and methods. WHP Office Report WHPO 91-1, WOCE Report No. 68/91, Woods Hole, Mass, USA.

Dickson, A.G., Sabine, C.L., and Christian, J.R. (Eds.) 2007. Guide to best practices for ocean CO_2 measurements. PICES Spec. Publ. 3, 191 pp.

Di Lorenzo, E. and Mantua, N. 2016. Multi-year persistence of the 2014/15 North Pacific marine heatwave. Nature Clim. Change 6: 1042–1047, https://doi.org/10.1038/nclimate3082

Di Lorenzo, E., Schneider, N., Cobb, K.M., Franks, P.J.S., Chhak, K., Miller, A.J., McWilliams, J.C., Bograd, S.J., Arango, H., Curchitser, E., Powell, T.M., and Rivière, P. 2008. North Pacific Gyre Oscillation links ocean climate and ecosystem change. Geophys. Res. Lett. 35: https://doi.org/10.1029/2007GL032838

Freeland, H. 2007. A short history of Ocean station Papa and Line P. Prog. Oceanogr. 75: 120–125, https://doi.org/10.1016/j.pocean.2007.08.005

Hamme, R.C., Webley, P.W., Crawford, W.R., Whitney, F.A., DeGrandpre, M.D., Emerson, S.R., Eriksen, C.C., Giesbrecht, K.E., Gower, J.F.R., Kavanaugh, M.T., Peña, M.A., Sabine, C.L., Batten, S.D., Coogan, L.A., Grundle, D.S., and Lockwood, D. 2010. Volcanic ash fuels anomalous plankton bloom in subarctic northeast Pacific. Geophys. Res. Lett. 37: L19604, https://doi.org/10.1029/2010GL044629

Mackas, D.L., Thomson, R.E., and Galbraith, M., 2001. Changes in the zooplankton community of the British Columbia continental margin, 1985-1999, and their covariation with oceanographic conditions. Can. J. Fish. Aquat. Sci. 58: 685–702, https://doi.org/10.1139/f01-009

Mackey, M.D., Mackey, D.J., Higgins, H.W., and Wright, S.W. 1996. CHEMTAX - a program for estimating class abundances from chemical markers: application to HPLC measurements of phytoplankton. Mar. Ecol. Prog. Ser. 144: 265–283, doi:10.3354/meps144265

Mantua, N.J., Hare, S.R., Zhang, Y., Wallace, J.M., and Francis, R.C. 1997. A Pacific decadal climate oscillation with impacts on salmon. Bull. Amer. Meteorol. Soc. 78: 1069–1080, https://doi.org/10.1175/1520-0477(1997)078<1069:APICOW>2.0.CO;2

Peña, M.A., Nemcek, N., and Robert, M. 2019. Phytoplankton responses to the 2014–2016 warming anomaly in the northeast subarctic Pacific Ocean. Limnol. Oceanogr. 64: 515–525, https://doi.org/10.1002/lno.11056

Whitney, F.A., Freeland, H.J., and Robert, M. 2007. Persistently declining oxygen levels in the interior waters of the eastern subarctic pacific. Prog. Oceanogr. 75: 179–199, https://doi.org/10.1016/j.pocean.2007.08.007